Dielectric Properties of Sustainable Nanocomposites Based on Zein Protein and Lignin for Biodegradable Insulators

Maria Oliviero, Reza Rizvi, Letizia Verdolotti, Salvatore Iannace, Hani E. Naguib, Ernesto Di Maio, Heinz C. Neitzert, and Giovanni Landi*

Two types of lignin, alkali lignin and lignosulfonic acid sodium salt, are blended into thermoplastic zein through melt mixing in order to develop biodegradable insulator materials for multifunctional applications in electronics. The effects of lignin type and content on the dielectric properties of the resulting bio-nanocomposites are investigated. The results indicate that, by modifying the structural arrangement of the zein with the use of lignin, it is possible to obtain bio-nanocomposites characterized by tunable dielectric properties. The bio-nanocomposites containing low amounts of lignin derivatives exhibit extensive protein structural changes together with a modification of the dielectric properties compared to the pristine thermoplastic zein. Changes in the dielectric properties of these systems are also observed to change over time, indicating a loss of plasticizer, as is evident by a decrease in the glass-transition temperature. At high frequencies, the resulting values of the dielectric permittivity and of the loss tangent demonstrate that the bio-nanocomposite can be used as biodegradable dielectric material for transient (temporary) electronics.

1. Introduction

In recent years, the electronic industry has put considerable efforts to improve its environmental profile, primarily by optimizing the energy efficiency of products and devices, and the use of sustainable materials.[1] Biopolymers can be used as alternatives to synthetic polymers in a number of engineering applications such as temperature sensors and development of scaffolds for tissue engineering.[2,3] In particular, the use of biopolymers from renewable resources in the field of biodegradable electronics, may offer a number of advantages, especially eco-friendliness and ease of disposability, increased functionality, nontoxicity, increased design flexibility, and, possibly, reduced unit cost.[4,5] Throughout history, natural polymers have been used as alternative packaging materials with lower environmental impact.[6] However, only in recent years several applications in the consumer electronics such as energy power sources,[7] temporary biomedical implants,[8] and zero-waste biosensors[9] have been implemented with the aim of using these natural materials alone, or in heterogeneous configurations with semiconducting materials.[10] Many natural polymers demonstrate excellent dielectric properties, which, combined with low-temperature processing, make them particularly suited as gate electrode insulators for field effect transistor applications.[11,12]

Petritz et al. have developed an organic complementary inverter based on hybrid dielectric composed of a bilayer of alumina and an ultrathin natural-source-cellulose layer characterized by a high electrical robustness against breakdown and sufficiently high-frequency stability.[13] Capelli et al. have used the silk protein as a thin film dielectric in an organic thin film field-effect transistor and in an organic light-emitting transistor.[14] Traditionally, dielectric materials are inorganic compounds, for example, mica and SiO_2.[15] Polymers are more flexible and offer excellent processability,[16,17] although they typically possess insufficient thermal conductivity and dielectric properties compared to inorganic compounds.[18] To overcome these limits, inorganic fillers are added to the polymeric matrix (composites or nanocomposites).[19]

The obtained composite/nanocomposites represent a new and interesting alternative to traditional dielectric materials in the electronic device fabrication,[20] with special sustainability feature when both polymeric matrix and filler are obtained from sustainable sources. Yu et al. have synthesized an eco-friendly dielectric material made from natural graphite and biodegradable poly(butylene succinate) having a high dielectric constant compared to the pure biopolymer matrix for energy storage applications.[21] Recently, biopolymers such as silk, gelatin, and cellulose derivatives have been reported in literature as a

Dr. M. Oliviero, Dr. L. Verdolotti, Dr. G. Landi
Institute for Polymers, Composites and Biomaterials (IPCB) – CNR
P.le E. Fermi 1, 80055 Portici, Naples, Italy
E-mail: letizia.verdolotti@cnr.it
Prof. R. Rizvi, Dr. H. E. Naguib
Department of Mechanical and Industrial Engineering
University of Toronto
184 College St., Toronto, ON M5S 3E4, Canada
Dr. S. Iannace
Institute for Macromolecular Studies (ISMAC) – CNR
Via E. Bassini 15, 20133 Milano, Italy
Prof. E. Di Maio
Department of Chemical, Materials and Production Engineering
University of Naples Federico II
P.le Tecchio 80, 80125 Naples, Italy
Prof. H. C. Neitzert, Dr. G. Landi
Department of Industrial Engineering
University of Salerno
Via Giovanni Paolo II 132, 84084 Fisciano, SA, Italy

DOI: 10.1002/adfm.201605142

biodegradable material for transient devices and systems.[1,7,22] Transient electronics are devices that can dissolve into the surrounding environment with minimal or nontraceable remains after a period of stable operation.[1] Rogers and co-workers have fabricated a working device that includes transistors, diodes, capacitors, and resistors with interconnects and interlayer dielectrics, all on a thin silk substrate.[23] In this system, MgO, SiO_2, and SiN_x are used as dielectrics and encapsulating layers, and synthetic biodegradable polymers (e.g., silk, poly(lactic-*co*-glycolic acid) (PLGA), polycaprolactone (PCL), poly(lactic acid) (PLA)) are used as substrates and packaging materials.[1]

In this respect, naturally occurring proteins and some polysaccharides, are generally considered biodegradable materials.[24,25] However, their biodegradation rate can be modified by either chemical modifications or filler additions. In general, a strong reduction in biodegradation rate is expected when extensive cross-linked reactions (i.e., production of numerous covalent bonds between the polymer chains) are promoted.[26] Conversely, the addition of inert fillers can increase the biodegradation rate of a polymer matrix because its presence breaks the co-continuity of the polymer (increase the surface area and/or change the hydrophilic/hydrophobic ratio of the matrix).[27–29]

Zein, a prolamin (cereal storage protein) of corn, has proven as a potential candidate for replacing oil-based plastics, as it: i) can be extracted from the byproducts of the brewing and biofuel industries, ii) has excellent film-forming ability, and iii) possesses unique hydrophobicity, which is due to the high content of nonpolar amino acids.[30] Like any other protein, upon isolation from the native state, zein exhibits high density and brittle behavior, with a high modulus and stress to break and a low strain to break. Plasticization, a common method to improve polymer deformability, can then be adopted, in this case with the use of small polar molecules such as water, glycerol, and ethylene glycol.[31]

Thermoplasticization, a process when plasticization is conducted with the additional use of heat and shear forces, induces a modification of the native supramolecular arrangement of the protein and, in particular, its secondary structure. The secondary structure of the proteins can be formally defined by the pattern of hydrogen bonds between local segments of polypeptide chains. The most common secondary structures of zein are α-helices and β-sheets shown in **Figure 1**. The protein–protein hydrogen-bonds weakening and the increase of free volume and molecular mobility are the mechanisms proposed in the literature[30,31] for describing the effects induced by the thermoplasticization process and are responsible for the definition of the final properties of the biopolymer. Furthermore, it has been shown that the presence of nanometric fillers into the biopolymer (bio-nanocomposite) has an additional role in defining the secondary structure and hence the final macromolecular conformation. For this reason, the final material performances of the bio-nanocomposites are affected by the presence of the nanometric additive to a larger extent when compared with oil-based traditional plastics.[32,33]

Lignin is an amorphous biopolymer, largely a constituent of woody plant biomass, and a byproduct from several biomass processing industries. Currently, lignin is primarily used as a low-cost fuel for biomass energy generation.[34] From the chemical point of view, lignin can be defined as a very reactive

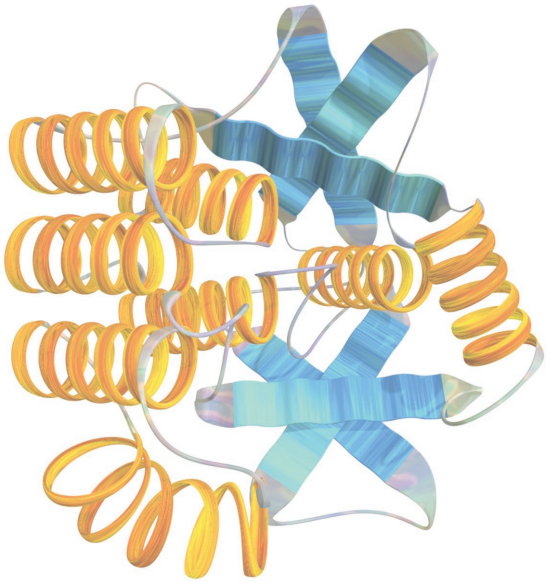

Figure 1. Secondary structure of zein (α-helices and β-sheets).

macromolecular compound, because of its functional groups such as aromatic rings, phenolic and aliphatic alcohol groups, and methoxy groups; all being possible sites for chemical modifications and/or reactions.[32]

In this respect, other main applications include the use of lignin as renewable chemicals,[35] bio-polyol source to synthesize polyurethanes foams,[36] filler for improving the performances of thermoplastic elastomer,[37] partially renewable matrix for composites,[38] and as precursor for carbon materials.[39–41]

Previously, we have introduced thermoplasticized zein by melt mixing,[42] and probed the role of both the molecular architecture of the protein and the nature of plasticizers on the chemo-physical properties and the ability to withstand extreme elongational deformation during film processing.[43] More recently, zein-based nanocomposites with lignin derivatives have been developed and the interactions among the protein, the plasticizers, and the lignin derivatives analyzed to explain the protein structural changes and conformational modifications brought about by the lignin derivatives.[32–44] Such modifications resulted in the improvement of mechanical, water sorption, and flame-retardant properties[32,43,44] paving the way to further exploitation of the materials in the emerging field of the biodegradable electronics.

Here, we analyze how the complex mechanism of interactions of zein molecules with a plasticizer (poly(ethylene glycol) (PEG)) and two types of lignin derivatives (alkali lignin, AL, and lignosulfonic acid sodium salt, LSS) influence the dielectric response of the produced bio-nanocomposites.

In order to evaluate the aging of the bio-nanocomposites, the dielectric and electrical properties, after 48 h and after six months, have been compared. Because long-term changes of dielectric properties depend essentially on migration of the PEG plasticizer, glass-transition temperature changes have also been monitored by a dynamic mechanical analysis (DMA).

In this respect, the zein-based nanocomposite can be used as biodegradable substrate (instead of silk) and also as a packaging material instead of synthetic polymers (i.e., PLA, PLGA, and PCL) in the biodegradable/transient electronic systems.

Lignin additives did not cross-link (through covalent bonds) to the zein structure, for that it is not expected to affect significantly the biodegradation rate of the zein matrix.

Moreover, given that the addition of the lignin filler into the zein matrix leads to a tuning of the dielectric properties, the thermoplastic zein-based bio-nanocomposites with two different lignin derivatives can be considered as a possible material for gate and interlayer dielectric material.

These promising results highlight the potential for use of zein-based bio-nanocomposites as dielectric material in the field of biodegradable electronics for transient applications.

2. Results and Discussion

2.1. Dielectric Properties

Dielectric impedance spectroscopy is an important electrical characterization technique, which can provide charge polarization information and insights into free and bound charges in a material. The permittivity spectrographs for pristine thermoplastic zein (TPZ) and TPZ-based bio-nanocomposites containing various amounts of AL and LSS are illustrated in **Figure 2**a,b, respectively. Starting at high frequencies (10^5 Hz), the permittivity of TPZ gradually increases as the applied frequency is reduced. At frequencies below 10 Hz, TPZ undergoes a low-frequency dispersion (LFD), marked by a rapid increase in permittivity. The LDF behavior in hydrophilic proteins has been attributed either to the Maxwell–Wagner effect (Ω-dispersion) or to proton and impurity ion conduction (α-dispersion).[45,46] The Maxwell–Wagner dispersion is prominent at high charge carrier concentrations, when mobile charges accumulate at sample–electrode interfaces as well as at any internal interfaces in heterogeneous materials. The polarization resulting from charge accumulation at interfaces may have significant contributions to the observed high dielectric permittivity, ε', which scales with frequency as $\varepsilon' \propto \omega^{-2}$, and high dielectric loss, ε'' which scales with frequency as $\varepsilon'' \propto \omega^{-1}$.[47] In contrast, the proton and impurity ion conduction results from charge carrier hopping across a lattice of surface absorbed water molecules. Through percolation dynamics, the absorbed water molecules can form a network of hydrogen bonds,[48] which can facilitate the long-range hopping motion of protons. The proton hopping mechanism is activation energy driven,[49] therefore it is highly dependent on temperature, whereas the hydrogen bonded network forms through a percolation process[50] depending on the hydration level. Proton conduction may also result in high dielectric permittivity and loss values with the scaling behavior showing either individual or both dispersion processes. The dispersion phenomena observed in TPZ (Figure 2) has an ε' with an exponent of −1.44 and an ε'' with an exponent of −0.95 indicating a composite mode of low-frequency dispersion where both charge accumulation at interfaces and lattice hopping of protons are occurring simultaneously. In contrast, the addition of AL (Figure 2a) reduces the dispersion behavior, as indicated by the lower values of ε' and slope at low frequency. At a AL content of 10 wt%, the frequency scaling behavior of the dielectric ε' and ε'' are −1.12 and −1.00, respectively, which are close to unity and similar in magnitude, thereby indicating the dominance of proton conduction in the bio-nanocomposites. The addition of LSS (Figure 2b) to the TPZ has a minor effect in reducing the dispersion behavior. The slopes for the ε' (≈1.5) and ε'' (≈1) are close to the TPZ case, as do the magnitudes of the dispersion behavior, indicating a composite dispersion process consisting of both proton hopping and Maxwell–Wagner interfacial polarization. The absence of the Maxwell–Wagner interfacial polarization observed for TPZ-based bio-nanocomposites with high amount of AL indicates a lower conductivity through reduced charge carrier concentration or mobility. This is further confirmed by the electrical conductivity, σ', acquired from the impedance measurements (**Figure 3**). At high frequencies, the conductivity behavior of pristine TPZ is frequency dependent, proving to be an insulating dielectric material. In contrast, at low frequencies, conductivity becomes frequency independent, suggesting the presence of mobile charge carriers, which can be protons as well as impurity ions. In the case of TPZ σ' is 5×10^{-9} S cm^{-1}, with an onset of frequency independent charge transport (f_{on}) at ≈500 Hz. The addition of lignin (AL and LSS) in different amounts induces interesting changes in the σ' of TPZ-based bio-nanocomposites, and two cases can be distinguished: low (1 and 3 wt%) and high (5 and 10 wt%) lignin content. In particular, at low lignin content,

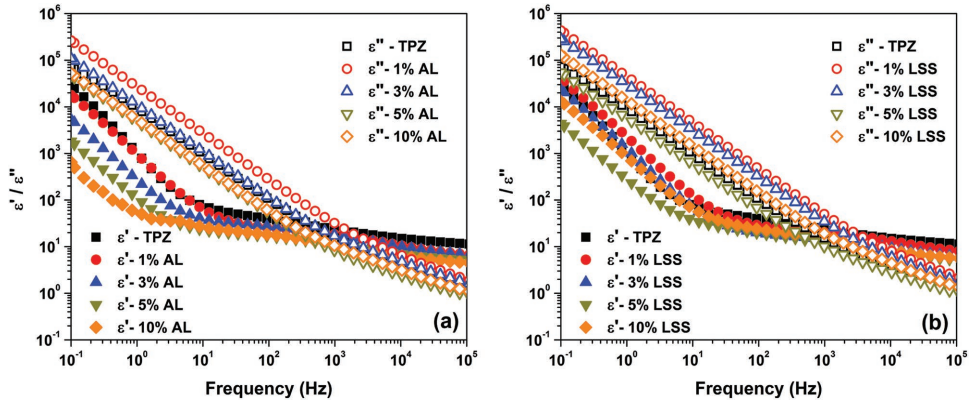

Figure 2. ε' and ε'' of TPZ and TPZ-based bio-nanocomposites: a) bio-nanocomposites with AL; b) bio-nanocomposites with LSS.

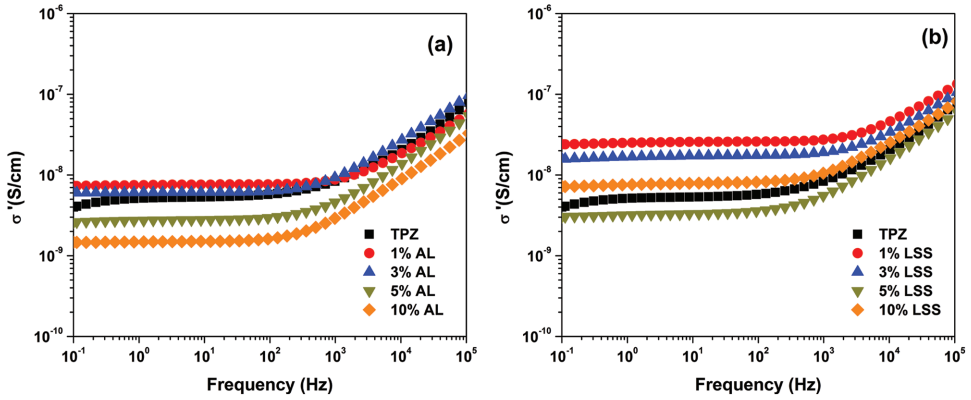

Figure 3. The electrical conductivity σ' of TPZ and TPZ-based bio-nanocomposites: a) bio-nanocomposites with AL; b) bio-nanocomposites with LSS.

samples presented a slight increase of σ' with respect to pristine TPZ. In view of the results from the Fourier transform infrared spectroscopy (FTIR) and the X-ray diffraction (XRD) analyses reported by Oliviero et al.,[32] we may infer that these behaviors (see **Figure 4**a) are governed by a new arrangement of interhelix packing of zein, with an insertion of the lignin macromolecule within the zein layers and formation of H-bonds between the functional groups (OH, SH) of lignin and the functional groups of zein (C=O, OH, RNH). Given that the lignin has a lower dielectric constant than TPZ,[51,52] according to the Maxwell–Garnet theory,[53] the presence of the second lignin-rich phase with lower dielectric constant in the bio-nanocomposite produces a marked decrease of the overall dielectric constant. It is worth noting that the alkali reduction of the lignin phase produces a further decrease of the ε' at low frequencies.[54,55] Moreover, the formation of a network of hydrogen bonds facilitates the long-range hopping motion of protons (see Figure 4b) with a consequent increase of σ'. Conversely, samples with higher AL content (Figure 3a) shows a decrease of σ'. For example, at 10 wt% AL content, $\sigma' = 1 \times 10^{-9}$ S cm^{-1} at $f_{on} \approx 100$ Hz have been measured. The lower ε' and σ' in the TPZ-based bio-nanocomposites containing high amounts of AL are attributed, as shown in **Figure 5**, to a certain degree of phase separation between the lignin-rich phase and the zein phase, as observed by transmission electron microscopy (TEM) analysis, that reduces the charge mobility (see Figure 5b). For instance, TEM image of TPZ filled with high amounts of AL (10 wt% of AL),[56,57] shown in Figure 5c, highlights the presence of inhomogeneous morphology with clear zones alternate to denser-black domains. The clear domains may be ascribed to the segregation of PEG between zein macromolecules while the dense domains (ranging from 20 to ≈80 nm sized) dispersed within the matrix consist of AL aggregated particles distributed throughout the sample surface as schematized in Figure 5a,b.

In comparison, the addition of LSS (Figure 3b) did not affect the ε' and σ', having in this case a slightly higher value of σ' of 7×10^{-9} S cm^{-1} and an onset frequency at ≈500 Hz for the sample containing 10 wt% LSS, due to the presence of the sodium atoms in the filler.

Figure 6 compares the dielectric permittivity and the dielectric loss tangent ($\varepsilon''/\varepsilon'$) of the TPZ bio-nanocomposite with different filler contents of AL and LSS. As can be observed in Figure 6a, at low frequencies the effect of the lignin derivatives on the ε' is strongly evident. The high value assumed by the ratio $\varepsilon''/\varepsilon'$ can be related to the charge accumulation at interfaces or to the proton and impurity ion conduction in the bio-nanocomposites. Conversely, at high frequencies the dielectric loss tangent has a value of about 0.1 for both the filler types used, as can be observed in Figure 6b. This value is in good agreement with that found in literature for alternative biodegradable system such as poly(butylene succinate).[21] It is worth noting that the synthetic biopolymers show lower values of the

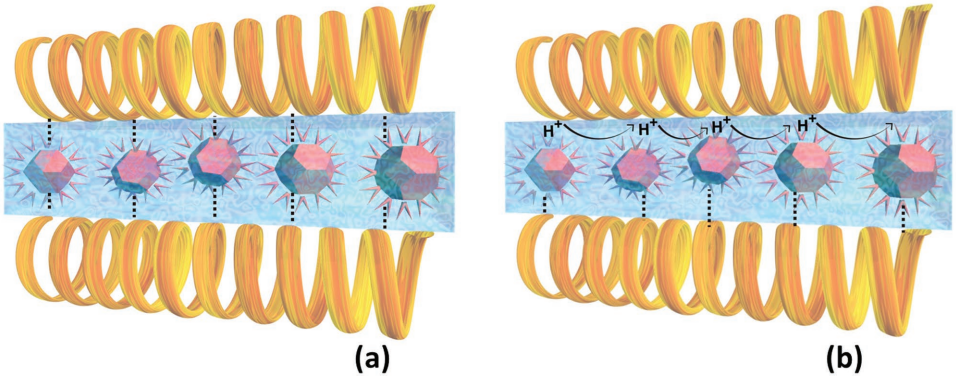

Figure 4. Schematic representation of the secondary structure of zein protein after thermoplasticization with a low AL content. a) Insertion of PEG and lignin (AL or LSS) between the α-helixes and b) long-range hopping motion of protons along the hydrogen network.

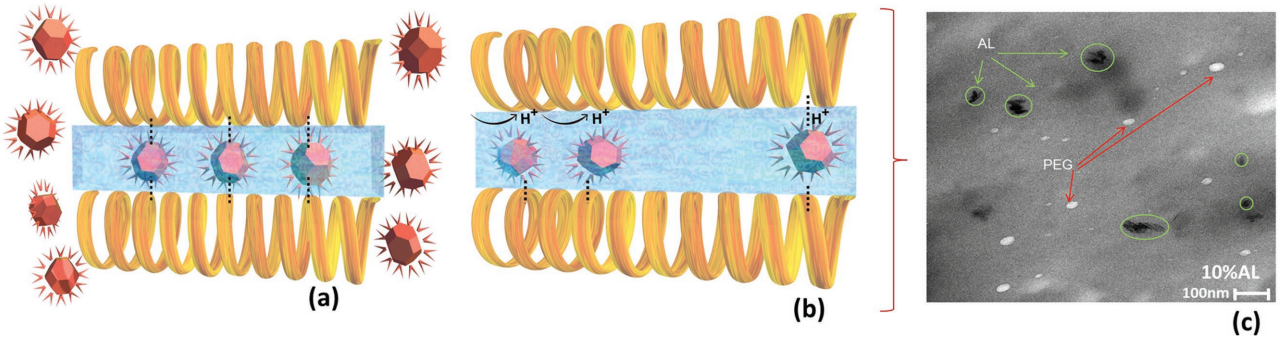

Figure 5. Schematic representation of the secondary structure of zein protein after thermoplasticization with a high AL content. a) Insertion of PEG and AL between the α-helix and phase separation between zein and a certain amount of AL and b) discontinuity of long-range hopping motion of protons along the network of hydrogen. c) TEM image of TPZ filled with high AL content, 10 wt%.

dielectric loss tangent ranges between 10^{-3} and 10^{-1}.[13] In this frequency range, it can be assumed that $\varepsilon' \approx \varepsilon_r$, where ε_r represents the relative dielectric constant assuming that the dielectric loss tangent is negligible. Therefore, for a low concentration of the lignin derivatives (i.e., 1 and 3 wt%) the permittivity value of the bio-nanocomposite can be tuned by changing the weight fraction of the filler, without phase separation between the filler and zein-plasticizer phase. In particular, the pristine TPZ shows a value of $\varepsilon_r \approx 7$ and decrease as the increase of the filler down to a value of about 5 with a filler concentration of 3%. These values are in good agreement with those found in literature for the used dielectric materials in transient systems.[1–13]

2.2. Aging

The current density–voltage characteristics (J–V), measured in the range between ±100 V, of the TPZ and TPZ-based bio-nanocomposites loaded with 1 and 10 wt% of the AL or LSS, after an aging period of six months are shown in **Figure 7**a,b, respectively. The J–V characteristics of the other compositions are similar and have been reported in the Supporting Information (Figure S1, Supporting Information). The measurements have been performed by applying a bias voltage, which increases with a scan rate of 1.5 V s^{-1} in the forward and backward direction. Under these conditions, the slope of the J–V curves gives the conductivity, σ_{DC}, and the hysteresis observed in the dc electrical measurements, is a clear indication of the dielectric properties of the bio-nanocomposites after the aging time.

A comparison of the σ_{DC} values for the samples fresh (after 48 h from mixing) and aged (after six months) can be performed by considering that for frequencies below f_{on}, the σ' remains almost constant, as shown in **Figure 8**. These values, for both the filler types, can be compared with the slopes extracted from the J–V characteristics, displayed in Figure 7a,b. By taking into account Equation (3) and (4) reported in the Experimental Section, the value of ε' can be calculated from the J–V curves for a frequency of 1.5 Hz and compared with the data reported in Figure 2a,b for the same frequency.

In Figure 8a,b, a comparison of the σ_{DC} values, for fresh TPZ and TPZ-based bio-nanocomposites as a function of the lignin content (AL and LSS) and aged, is shown. As already observed in Figure 3, the fresh samples show σ_{DC} values ranging between 10^{-8} and 10^{-9} S cm^{-1} and 10^{-7} and 10^{-9} S cm^{-1} for the AL and LSS, respectively. After the aging period, a marked decrease of about four orders of magnitude of the conductivity values can be observed. In particular, the value of σ_{DC} for the fresh TPZ reduces to 0.61×10^{-12} S cm^{-1}. The insertion of 1 wt% of filler into the biopolymer matrix also causes a slight increase of the σ_{DC} value up to 0.69×10^{-12} and 0.87×10^{-12} S cm^{-1} for the AL and LSS lignin, respectively. Conversely, with a concentration of the 10 wt% a minor decrease of the electrical conductivity down

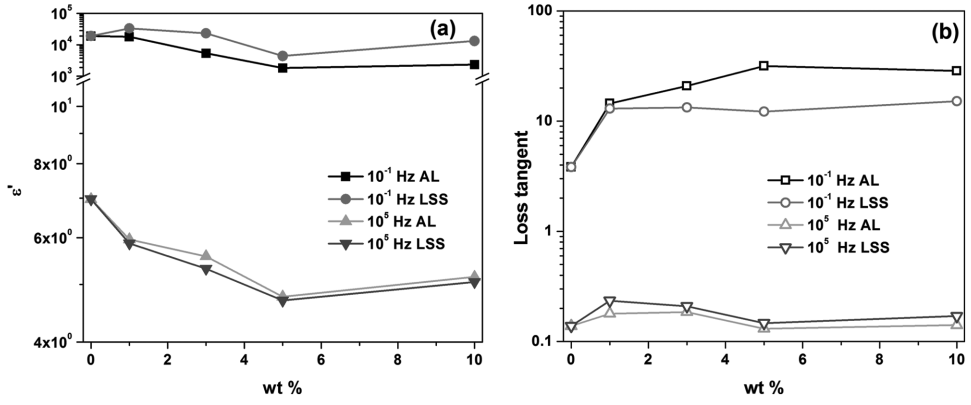

Figure 6. Dependence of a) ε' and b) dielectric loss tangent of TPZ-based bio-nanocomposites on the weight fraction of AL or LSS at 10^{-1} Hz and 10^5 Hz, respectively.

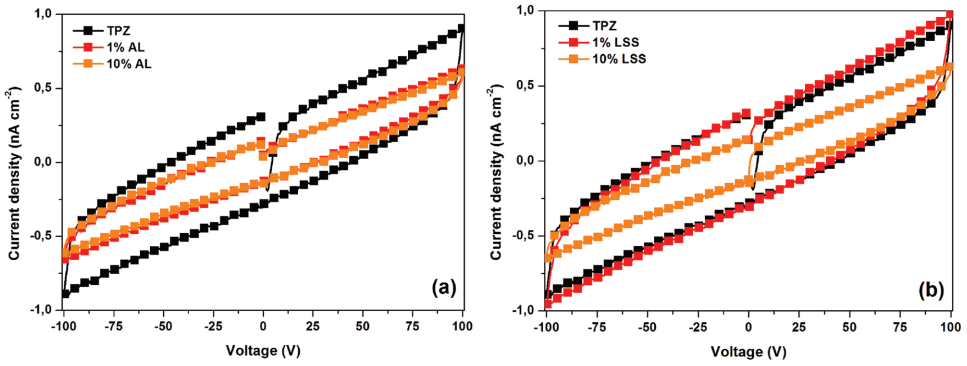

Figure 7. Current-density–voltage characteristics of aged TPZ and TPZ-based bio-nanocomposites containing 1 and 10 wt% of a) AL and b) LSS.

to 0.47×10^{-12} and 0.37×10^{-12} S cm^{-1} has been observed for both lignin systems (AL and LSS). The lowest value of σ_{DC} for the aged materials can be related to the migration of the plasticizer within the bio-nanocomposites.

In **Figure 9**a,b, a comparison between the ε' extracted from the *J–V* curves for the fresh and aged TPZ-based bio-nanocomposites, as a function of the filler contents of AL and LSS is shown. In contrast to the σ_{DC} behavior displayed in Figure 8, the diffusion out of the plasticizer leads to an increase of the dielectric permittivity values for both AL and LSS. For the TPZ sample, aging causes a fivefold increase of ε'. A clear indication of the role played by the fillers, on migration of the PEG molecules, can be drawn by considering the different values of ε' between the fresh and aged samples. As already mentioned, for the sample with low amount of AL (1 and 3 wt%), the filler creates H-bonds between the functional groups of lignin and the functional groups of the zein. On the other hand, the addition of the 5 and 10 wt% AL causes a phase separation in the blend, with a consequent worsening of the dielectric properties. As a consequence, changes within the composite structure (as results by the FTIR and XRD spectra reported in ref. [32]) influence the dielectric and electrical properties of the sample after 48 h.[32] The formation of a network of hydrogen bonds modifies the diffusion of the PEG molecules within the sample during the aging treatment. This finding can be observed in Figure 9a, with a small increase (about three times) of the ε' value, compared to the samples with 1 wt% of AL, where the increase (after aging of six months) is about 40-fold with respect to the bio-nanocomposite with 10 wt% of AL. The major increase of ε' value for the sample with 5 and 10 wt% of AL can be related to the presence of two distinct phases within the bulk material. In this case, the migration of the plasticizer becomes more supported as a consequence of the reduced amount of H-bonds.

For the polymer matrix loaded with different LSS content, small differences between ε' values for the fresh and aged samples have been observed, indicating that the filler does not modify the migration of the plasticizer. This result confirms that, in such a system, even after 48 h, a strong segregation between the filler and the plasticizer is occurring in the sample. It is worth noting that ε', observed for the bio-nanocomposites loaded with 10 wt% of AL and LSS, shows the same value for both the filler types. This result is a further indication that a phase separation between the filler and the zein-plasticizer phase occurs within the blend. Moreover, after the phase separation, the electrical and dielectric properties result to be more influenced by the biopolymer rather than by the filler.[58,59]

The variation of the plasticizer amount within the TPZ-based bio-nanocomposites over time has also been evaluated by monitoring in parallel the variation of glass-transition temperature, T_g, by DMA measurements. The T_g of samples has been determined as the temperature corresponding to the maximum of the tan δ peak.[32,60] The effect of the lignin (AL and LSS) addition and of the aging on T_g of TPZ is shown in **Figure 10**. When a low content of AL or LSS (1 wt%) is added, tan δ peak shifts to

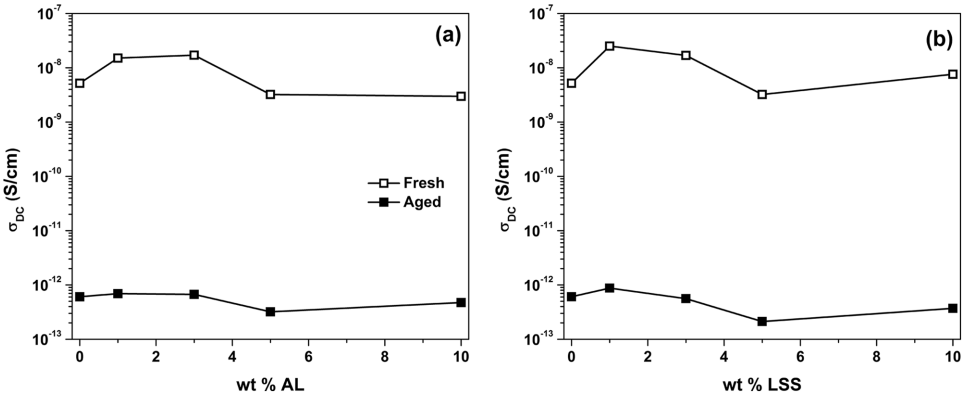

Figure 8. Comparison of the σ_{DC} of TPZ-based bio-nanocomposites as a function of the weight fraction of a) AL and b) LSS fresh (open symbols) and aged (closed symbols).

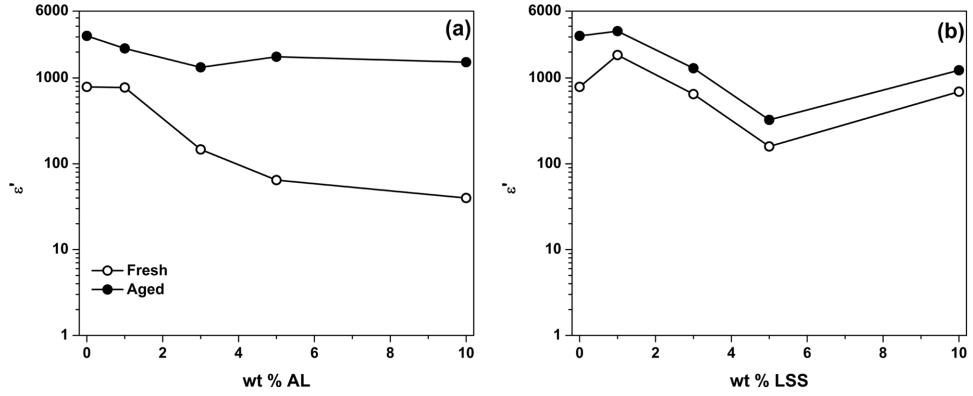

Figure 9. Comparison of the ε' of TPZ-based bio-nanocomposites as a function of the weight fraction of: a) AL and b) LSS fresh (open symbols) and aged (closed symbols).

lower temperatures. Further increase in the concentration of AL or LSS (to 10 wt%) is accompanied by peak shifting to higher temperatures. This finding may be due to the fact that the introduction of a small amount of lignin (AL and LSS) entails violation of the system of intra- and intermolecular hydrogen bonds that is typical for zein; that is, primary hydroxyl groups become more accessible. As also reported by Mizuno et al.,[61] the intermolecular interactions may prevent the local molecular motion; therefore, when these interactions are reduced, the mobility of TPZ-based bio-nanocomposites might increase with a corresponding shift of T_g toward lower temperatures. In particular, the authors related T_g depression of soy proteins cross-linked by microbial transgutaminase (MTG) treatment to the modification of the state of the secondary structure of the protein, especially to the disruption of the β-structure induced by MTG treatment. As the content of lignin is increased further (to 10 wt%), a certain degree of phase separation between the lignin-rich phase and zein phase occurs, restricting the segmental mobility of the protein chains in the vicinity of the lignin fragments and the value of T_g increases. After aging of six months the T_g of all systems increase due to migration of the PEG 400. The lower concentration of plasticizer in the TPZ-based bio-nanocomposites is responsible for lower local chain flexibility and for the lower conductivity.

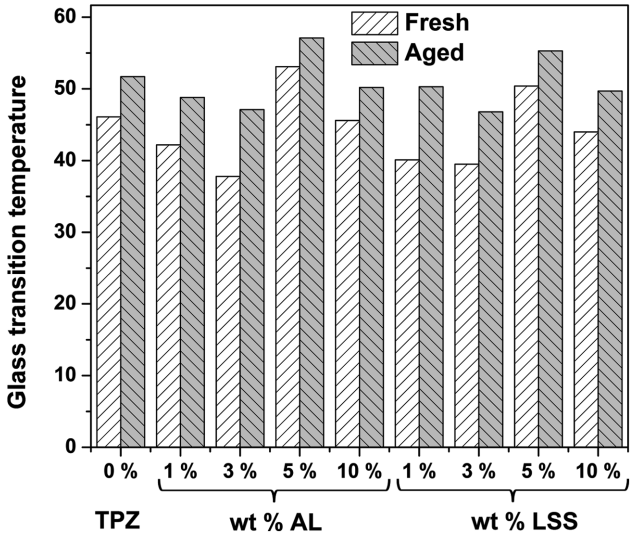

Figure 10. Glass-transition temperature (T_g) for TPZ and TPZ-based bio-nanocomposites with AL and LSS fresh (white bars) and aged (gray bars) at RH = 50%.

3. Conclusions

Thermoplastic zein-based bio-nanocomposites with two different lignin systems, alkali lignin and lignosulfonic acid sodium salt, have been developed through melt mixing and subsequently processed into films by using a compression molding. The results proved that, by modifying the structural arrangement of the zein with the use of a highly interactive additive such as lignin, it is possible to tune the dielectric properties of the bio-nanocomposite. At low frequencies, by increasing the alkali lignin content a reduction of the permittivity has been observed. On the contrary, the addition of the lignosulfonic acid sodium salt causes a strong phase separation in the blend with minor changes of the dielectric properties. At high frequencies, the dielectric permittivity value of the bio-nanocomposite varies between 5 and 7 as a function of the lignin derivatives content. Additionally, the dielectric loss tangent shows a value of about 0.1 for both the used fillers. Changes in the dielectric properties of these systems have also been studied over time. After a six months' aging period an increase of the dielectric response combined with a strong reduction of the electrical conductivity has been observed for all the investigated filler types. This effect can be related to the migration of the PEG plasticizer within the bio-nanocomposites, as highlighted by a reduction of the glass-transition temperature. The results presented here indicate that the thermoplastic zein-based bio-nanocomposites can be used as biodegradable dielectric material for transient electronics.

4. Experimental Section

Materials: Corn zein powder (M_w = 25 000 Da, CAS 9010-66-6, lot 065K0110, Sigma–Aldrich, Italy) and PEG (M_w = 400 Da, CAS 25322-68-3, Sigma–Aldrich, Italy) were used to prepare TPZ. In order to investigate the effect of lignin on dielectric permittivity and electrical

conductivity of TPZ, two different lignin systems were used, namely, alkali lignin (average $M_w \approx 28\,000$, CAS 8068-05-1, Sigma–Aldrich, Italy), denoted as AL and lignosulfonic acid–sodium salt (average $M_w \approx 52\,000$, CAS 8061-51-6, Sigma–Aldrich, Italy), denoted as LSS, with two different functional groups–thiol (—SH) for AL and hydroxyl (—OH) for LSS.

TPZ-Based Bio-Nanocomposites Preparation: TPZ-AL bio-nanocomposites were prepared by a two-step procedure including lignin derivatives dispersion in PEG solution and melt mixing process of zein+lignin derivatives+PEG. In particular, AL filler was first added to PEG in amount such that the final concentrations of AL were 1, 3, 5, and 10 wt% of the zein+PEG system (the amount of PEG was 25 wt% of the zein+PEG system), the resulting mixture was sonicated in ultrasonic bath (Labsonic FALC LBS2-15) with a frequency of 40 kHz and 100% output power at 35 °C under air atmosphere for 2 h. Subsequently, zein powder was added into the PEG+AL sonicated system and mixed in a beaker by hand to provide a crude blend and it was allowed to stand for 5 h at ambient temperature.

Subsequently, the crude blend was then subjected to temperature and shear stresses in a twin screw counter-rotating internal mixer (Rheomix 600) connected to a control unit (Haake PolyLab QC, Haake, Germany) for thermoplasticization. Mixing temperature, speed of rotation, and mixing time were 70 °C, 50 r min^{-1}, and 10 min, respectively.[32] The same procedure was used to produce the samples with LSS in place of AL and to produce TPZ for proper comparison. A P300P hot press (Collin, Germany) was then used to prepare thin films. Materials were heated to the same temperature of mixing and pressed at 50 bars for 10 min and subsequently cooled to 30 °C under pressure.

Before testing, film specimens were removed from the press and stored at room temperature and 50% relative humidity (RH). The first dielectric tests were carried out 48 h after the beginning of the storage period.

TPZ-Based Bio-Nanocomposites Characterization: Dielectric spectroscopy was performed through an Alpha L (Novocontrol Technologies, Germany) dielectric impedance analyzer. Thin disc samples, measuring 20 mm in diameter and a thickness of 1 mm, were clamped between two gold-coated electrodes in a shielded sample chamber. The impedance and phase information of the samples have been measured with a signal amplitude of 1 V (rms) frequencies of 10^{-1}–10^5 Hz. The sample's real and imaginary permittivity and conductivity can be obtained by modeling the material as an equivalent parallel RC circuit[62] whose impedance, Z^*, is defined as:

$$Z^* = \frac{1}{\frac{1}{R(\omega)} + i\omega C(\omega)} \tag{1}$$

where $R(\omega)$ and $C(\omega)$ are the sample's resistance and capacitance. Based on Equation (1), the complex permittivity, ε^* and conductivity, σ^*, of the sample is described by:

$$\varepsilon^*(\omega) = \frac{d\left(C^*(\omega) - C_0(\omega)\right)}{\varepsilon_0 A} = \frac{\sigma^*}{i\omega\varepsilon_0} \tag{2}$$

where d is the sample thickness, A is the sample area, ε_0 is the permittivity of free space, and C_0 is the capacitance of the empty cell.

The electrical measurements were performed in the voltage range between ±100 V after a six months' aging period on the samples in parallel configuration using a Keithley model "487" picoammeter and voltage source measurement unit (SMU). The films were electrically contacted by using gold tips to ensure a good ohmic contact with an average area (A) of 0.07 cm^2. The surface capacitance C_S (F cm^{-2}) was calculated integrating the area under the cyclic voltammograms (CVs) curves according to the following equation:[63]

$$C_S = \frac{1}{\vartheta \times A \times (V_B - V_C)} \int_{V_C}^{V_B} i(V)\, dV \tag{3}$$

where ν is the scan rate and $V_B - V_C$ is the applied potential window. The real part of the dielectric permittivity ε' has been calculated by using the equation:

$$\varepsilon' = \frac{C_S}{C_0} \tag{4}$$

where C_S is the measured capacitance and $C_0 = \varepsilon_0 \frac{A}{d}$ where d is the thickness of the sample and $\varepsilon_0 = 8.85 \times 10^{-14}$ F cm^{-1} the vacuum permittivity.[17] The AC electrical conductivity (σ') was calculated from the dielectric data using the equation:[64]

$$\sigma' = \sigma_{DC} + \omega\varepsilon_0\varepsilon'' \tag{5}$$

where ε'' is the imaginary part of the dielectric permittivity and the ω is the angular frequency (which is equal to $2\pi f$, where f is the frequency). It is worth noting that the dc electrical conductivity (σ_{DC}) can also be evaluated by taking into account the slope of the electrical characteristics in the voltage range of ±100 V on the sample in parallel configuration.[65]

The morphological structures of selected hybrid films (high concentration of AL) were characterized by using a TEM-100CX apparatus, manufactured by JEOL. Examinations were made on thin slices microtomed from cast films embedded in epoxy resin.

Dynamic mechanical tests were carried out by means of a DMA Tritec 2000 (Triton, UK) in tensile deformation. Samples were 20 mm long, 8 mm wide, and 0.5 mm thick, and the gauge length was 10 mm. Temperature scan tests were performed by applying a tensile amplitude of 10 µm at 1 Hz frequency and at heating rate of 3 °C min^{-1} from –80 to 100 °C. Three samples were analyzed for each lignin content after 48 h and after a six months' aging period.

Supporting Information

Supporting Information is available from the Wiley Online Library or from the author.

Acknowledgements

The authors gratefully acknowledge the graphical assistance of Dr. Enza Migliore.

Received: October 3, 2016
Revised: November 23, 2016
Published online: January 17, 2017

[1] K. K. Fu, Z. Wang, J. Dai, M. Carter, L. Hu, *Chem. Mater.* **2016**, *28*, 3527.
[2] R. Di Giacomo, B. Maresca, M. Angelillo, G. Landi, A. Leone, M. C. Vaccaro, C. Boit, A. Porta, H. C. Neitzert, *IEEE Trans. Nanotechnol.* **2013**, *12*, 1026.
[3] R. Di Giacomo, B. Maresca, A. Porta, P. Sabatino, G. Carapella, H. C. Neitzert, *IEEE Trans. Nanotechnol.* **2013**, *12*, 111.
[4] M. I. Vladu, E. D. Głowacki, P. A. Troshin, G. Schwabegger, L. Leonat, D. K. Susarova, O. Krystal, M. Ullah, Y. Kanbur, M. A. Bodea, V. F. Razumov, H. Sitter, S. Bauer, N. S. Sariciftci, *Adv. Mater.* **2012**, *24*, 375.
[5] A. Osswald, S. Garcia-Rodriguez, in *Handbook of Applied Biopolymer Technology*, Vol. *12*, (Eds: K. Sharma, A. Mudhoo), Royal Society of Chemistry, Cambridge, UK **2011**, p. 1.
[6] M. D. Sanchez-Garcia, L. Hilliou, J. M. Lagaron, *J. Agric. Food Chem.* **2010**, *58*, 6884.
[7] G. Landi, A. Sorrentino, F. Fedi, H. C. Neitzert, S. Iannace, *Nano Energy* **2015**, *17*, 348.

[8] Y. J. Kim, S. E. Chun, J. Whitacre, C. J. Bettinger, *J. Mater. Chem. B* **2013**, *1*, 3781.
[9] S. Hwang, C. H. Lee, H. Cheng, J. Jeong, S. K. Kang, J. Kim, J. Shin, J. Yang, Z. Liu, G. A. Ameer, Y. Huang, J. A. Rogers, *Nano Lett.* **2015**, *15*, 2801.
[10] C. Dagdeviren, S. W. Hwang, Y. Su, S. Kim, H. Cheng, O. Gur, R. Haney, F. G. Omenetto, Y. Huang, J. Rogers, *Small* **2013**, *9*, 3398.
[11] C. Y. Wang, C. Fuentes-Hernandez, J. C. Liu, A. Dindar, S. Choi, J. P. Youngblood, R. J. Moon, B. Kippelen, *ACS Appl. Mater. Interfaces* **2015**, *7*, 4804.
[12] M. Irimia-Vladu, *Chem. Soc. Rev.* **2014**, *43*, 588.
[13] A. Petritz, A. Wolfberger, A. Fian, T. Griesser, M. Irimia-Vladu, B. Stadlober, *Adv. Mater.* **2015**, *27*, 7645.
[14] R. Capelli, J. J. Amsden, G. Generali, S. Toffanin, V. Benfenati, M. Muccini, D. L. Kaplan, F. G. Omenetto, R. Zamboni, *Org. Electron.* **2011**, *12*, 1146.
[15] W. Volksen, R. D. Miller, G. Dubois, *Chem. Rev.* **2010**, *110*, 56.
[16] M. Ree, K. J. Chen, D. P. Kirby, N. Katzenellenbogen, D. Grischkowsky, *J. Appl. Phys.* **1992**, *72*, 2014.
[17] G. Maier, *Prog. Polym. Sci.* **2001**, *26*, 3.
[18] H. S. Lee, A. S. Lee, K. Baek, S. S. Hwang, in *Dielectric Material*, (Ed: M. A. Silaghi), InTech, Oradea, Romania **2012**, p. 59.
[19] G. Landi, F. Fedi, A. Sorrentino, H. C. Neitzert, S. Iannace, in *Times of Polymers (TOP) and Composites 2014: Proc. 7th Int. Conf. Times of Polymers (TOP) and Composites*, Vol. *1599*, AIP Publishing, Melville, NY, USA, **2014**, p. 202.
[20] D. Fragiadakis, E. Logakis, P. Pissis, V. Y. Kramarenko, T. A. Shantalii, I. L. Karpova, K. S. Dragan, E. G. Privalko, A. A. Usenko, V. P. Privalko, *J. Phys. Conf. Ser.* **2005**, *10*, 139.
[21] L. Yu, Y. Zhang, W. Tong, J. Shang, B. Shen, F. Lv, P. K. Chu, *RSC Adv.* **2012**, *2*, 8793.
[22] S.-W. Hwang, D.-H. Kim, H. Tao, T. Kim, S. Kim, K. J. Yu, B. Panilaitis, J.-W. Jeong, J.-K. Song, F. G. Omenetto, J. A. Rogers, *Adv. Funct. Mater.* **2013**, *23*, 4087.
[23] S.-W. Hwang, H. Tao, D.-H. Kim, H. Cheng, J.-K. Song, E. Rill, M. A. Brenckle, B. Panilaitis, S. M. Won, Y.-S. Kim, Y. M. Song, K. J. Yu, A. Ameen, R. Li, Y. Su, M. Yang, D. L. Kaplan, M. R. Zakin, M. J. Slepian, Y. Huang, F. G. Omenetto, J. A. Rogers, *Science* **2012**, *337*, 1640.
[24] G. Swift, *Acc. Chem. Res.* **1993**, *26*, 105.
[25] F. Kawai, *Adv. Biochem. Eng. Biotechnol.* **1995**, *52*, 151.
[26] L. Verdolotti, M. Lavorgna, M. Oliviero, A. Sorrentino, V. Iozzino, G. Buonocore, S. Iannace, *ACS Sustainable Chem. Eng.* **2014**, *2*, 254.
[27] S. K. Mohan, T. Srivastava, *J. Biochem. Technol.* **2010**, *2*, 210.
[28] K. Leja, G. Lewandowicz, *Pol. J. Environ. Stud.* **2010**, *19*, 255.
[29] Z. N. Azwa, B. F. Yousif, A. C. Manalo, W. Karunasena, *Mater. Des.* **2013**, *47*, 424.
[30] J. W. Lawton, *Cereal Chem.* **2002**, *79*, 1.
[31] J. W. Lawton, *Cereal Chem.* **2004**, *81*, 1.
[32] M. Oliviero, L. Verdolotti, E. Di Maio, M. Aurilia, S. Iannace, *J. Agric. Food Chem.* **2011**, *59*, 10062.
[33] G. Mensitieri, E. Di Maio, G. G. Buonocore, I. Nedi, M. Oliviero, L. Sansone, S. Iannace, *Trends Food Sci. Technol.* **2011**, *22*, 72.
[34] M. Imann, *Nature* **2014**, *516*, 28.
[35] T. D. H. Bugg, R. Rahmanpour, *Curr. Opin. Chem. Biol.* **2015**, *29*, 10.
[36] H. Nadji, C. Bruzzese, M. N. Belgacem, A. Benaboura, A. Gandini, *Macromol. Mater. Eng.* **2005**, *290*, 1009.
[37] C. D. Tran, J. Chen, J. K. Keum, A. K. Naskar, *Adv. Funct. Mater.* **2016**, *26*, 2677.
[38] K. Akato, C. D. Tran, J. Chen, A. K. Naskar, *ACS Sustainable Chem. Eng.* **2015**, *3*, 3070.
[39] D. Saha, Y. Li, Z. Bi, J. Chen, J. K. Keum, D. K. Hensley, H. A. Grappe, H. M. Meyerl, S. Dai, M. P. Paranthaman, A. K. Naskar, *Langmuir* **2014**, *30*, 900.
[40] M. Nar, H. R. Rizvi, R. A. Dixon, F. Chen, A. Kovalcik, N. D'Souza, *Carbon* **2016**, *103*, 372.
[41] O. Hosseinaei, D. P. Harper, J. J. Bozell, T. G. Rials, *ACS Sustainable Chem. Eng.* **2016**, *4*, 5785.
[42] E. Di Maio, R. Mali, S. Iannace, *J. Polym. Environ.* **2010**, *18*, 626.
[43] M. Oliviero, L. Verdolotti, I. Nedi, F. Docimo, E. Di Maio, S. Iannace, *J. Cell. Plast.* **2011**, *48*, 516.
[44] L. Verdolotti, M. Oliviero, M. Lavorgna, S. Iannace, G. Camino, P. Vollaro, A. Frache, *Polym. Degrad. Stab.* **2016**, *134*, 115.
[45] R. Pethig, *Annu. Rev. Phys. Chem.* **1992**, *43*, 177.
[46] R. J. Klein, S. Zhang, S. Dou, B. H. Jones, R. H. Colby, J. Runt, *J. Chem. Phys.* **2006**, *124*, 144903.
[47] L. A. Dissado, R. M. Hill, *J. Chem. Soc., Faraday Trans. 2* **1984**, *80*, 291.
[48] G. Careri, A. Giansanti, J. A. Rupley, *Proc. Natl. Acad. Sci. USA* **1986**, *83*, 6810.
[49] E. Marzec, W. Warcho, *Bioelectrochemistry* **2005**, *65*, 89.
[50] M. Suherman, P. Taylor, G. Smith, *J. Non-cryst. Solids* **2002**, *305*, 317.
[51] R. Shukla, M. Cheryan, *Ind. Crops Prod.* **2001**, *13*, 171.
[52] S. Admassie, T. Y. Nilsson, O. Inganas, *Phys. Chem. Chem. Phys.* **2014**, *16*, 24681.
[53] D. J. Bergman, D. Stroud, *Solid State Phys.* **1992**, *46*, 147.
[54] N. M. Barkoula, B. Alcock, N. O. Cabrera, T. Peijs, *Polym. Polym. Compos.* **2008**, *16*, 101.
[55] M. A. Esmeraldo, A. C. H. Barreto, J. E. B. Freitas, P. B. A. Fechine, A. S. B. Sombra, E. Corradini, G. Mele, A. Maffezzoli, S. E. Mazzetto, *BioResources* **2010**, *5*, 2478.
[56] Y. H. Deng, Y. F. Liu, W. J. Zhang, X. Q. Qiu, *Acta Phys.-Chim. Sin.* **2015**, *31*, 505.
[57] X. Wang, F. Wu, Y. Duan, Y. Wang, C. Hao, C. Ge, *RSC Adv.* **2016**, *6*, 65644.
[58] K. Dillip, R. N. Pradhan, P. Choudhary, B. K. Samantaray, N. K. Karan, R. S. Katiyar, *Int. J. Electrochem. Sci.* **2007**, *2*, 861.
[59] G. Landi, A. Sorrentino, S. Iannace, H. C. Neitzert, *Adv. Condens. Matter Phys.* **2015**, *1*, 2015.
[60] G. Galietta, L. Di Gioia, S. Guilbert, B. Cuq, *J. Dairy Sci.* **1998**, *81*, 3123.
[61] A. Mizuno, M. Mitsuiki, M. Motoki, K. Ebisawa, E. Suzuki, *J. Agric. Food Chem.* **2000**, *48*, 3292.
[62] E. Barsoukov, J. R. Macdonald, *Impedance Spectroscopy: Theory, Experiment, and Applications*, 2nd ed., Wiley, Hoboken, NJ, USA **2005**.
[63] A. J. Bard, R. L. Faulkner, *Electrochemical Methods: Fundamentals and Applications*, 2nd ed., Wiley, Hoboken, NJ, USA **2001**.
[64] G. Landi, H. C. Neitzert, A. Sorrentino, in *Times of Polymers (TOP) and Composites 2014: Proc. 7th Int. Conf. Times of Polymers (TOP) and Composites*, AIP Publishing, Melville, NY, USA, **2016**, p. 020165.
[65] G. Landi, C. Altavilla, P. Ciambelli, H. C. Neitzert, S. Iannace, A. Sorrentino, *AIP Conf. Proc.* **2015**, *1695*, 020044.